OPEN ACCESS
IOP Publishing
European Journal of Physics
Eur. J. Phys. **42** (2020) 015401 (11pp)
https://doi.org/10.1088/1361-6404/abc5fd

Superoscillations and the quantum potential*

M V Berry

HH Wills Physics Laboratory, Tyndall Avenue, Bristol BS8 1TL, United Kingdom

E-mail: asymptotico@bristol.ac.uk

Received 25 September 2020
Accepted for publication 29 October 2020
Published 16 November 2020

Abstract

For quantum or other waves that are band-limited, the quantum potential in the Madelung–Bohm representation vanishes on the boundaries of regions where the waves are superoscillatory (i.e. where they vary faster than any of their Fourier components). This connection is illustrated by calculations of the quantum potential zeros for a superoscillatory superposition of plane waves, and by Aharonov–Bohm waves.

Keywords: interference, Madelung–Bohm, wavefunction

(Some figures may appear in colour only in the online journal)

1. Introduction

Connections are of central importance in physics, and especially valuable in the teaching of our subject. My purpose here is to note an unexpected connection between two aspects of the geometry of waves.

The first concerns the Madelung–Bohm representation of the Schrödinger wavefunction [1, 2], where the quantum and classical momenta are governed by equations differing only by the quantum potential $Q(\boldsymbol{r})$. Recently, the zeros of $Q(\boldsymbol{r})$ have been explored [3], to investigate the significance of these hypersurfaces (points in 1D, curves in 2D, etc) and their possible interpretation as the most classical places in the wave.

The second is superoscillations [4, 5]: variations in a band-limited function that are faster than its fastest Fourier component. Where superoscillations occur, the function is very small, as the result of almost-perfect destructive of the Fourier components in its spectrum. Applications

*'Physics is not just Concerning the Nature of Things, but Concerning the Interconnectedness of all the Natures of Things', F C Frank retirement speech 1976.

of this mathematical phenomenon are currently being explored in several contexts, including microscopy, signal processing, and quantum measurement [6].

The connection is the following: in a wide class of cases, the quantum potential zeros have the alternative interpretation as the demarcation between regions where waves are superoscillatory and regions where they are not.

Section 2 contains a reprise of the Madelung–Bohm formalism, in order to derive a simple condition for the zeros of the quantum potential. For band-limited waves in a uniform medium, this reduces to a known condition for superoscillations. Section 3 explores the example of a wave in the plane $\boldsymbol{r} = (x, y)$ constructed by extending to y a function that is superoscillatory on the x axis. Section 4 calculates the quantum potential zeros in Aharonov–Bohm (AB) waves, and interprets these in terms of an extended notion of superoscillation. The concluding section 5 lists some historical threads underlying the connection reported here.

2. General theory

Band-limited quantum waves are a subset of solutions of the time-independent Schrödinger equation for a particle with charge q, mass m and energy E in scalar and vector potentials $U(\boldsymbol{r})$, $\boldsymbol{A}(\boldsymbol{r})$:

$$\frac{\left(-\mathrm{i}\hbar\nabla - q\mathbf{A}(\mathbf{r})^2\right)}{2m}\psi(\mathbf{r}) + U(\mathbf{r})\,\psi(\mathbf{r}) = E\psi(\mathbf{r})\,. \tag{2.1}$$

The Madelung–Bohm formalism [2] is a polar representation of the wavefunction, conveniently written as

$$\psi(\mathbf{r}) = R(\mathbf{r})\exp\left(\mathrm{i}\frac{S(\mathbf{R})}{\hbar}\right). \tag{2.2}$$

Substitution into (2.1), followed by standard manipulations, leads to the following two equations, equivalent to the real and imaginary parts of (2.1):

$$\nabla\cdot\left(R(\mathbf{r})^2\ \mathbf{p}_{\mathrm{K,qu}}(\mathbf{r})\right) = 0, \quad \frac{\left|\mathbf{p}_{\mathrm{K,qu}}(\mathbf{r})\right|^2}{2m} + Q(\mathbf{r}) = \frac{p_{\mathrm{K,cl}}^2(\mathbf{r})}{2m}. \tag{2.3}$$

Here the quantum potential, the quantum kinetic momentum vector and the magnitude of the classical kinetic momentum (mass times velocity), are defined by

$$\begin{aligned} Q(\mathbf{r}) &\equiv -\frac{\hbar^2\nabla^2 R(\mathbf{r})}{2mR(\mathbf{r})}, \\ \mathbf{p}_{\mathrm{K,qu}}(\mathbf{r}) &\equiv \nabla S(\mathbf{r}) - q\mathbf{A}(\mathbf{r}), \quad p_{\mathrm{K,cl}}(\mathbf{r}) \equiv \sqrt{2m\left(E - U(\mathbf{r})\right)}. \end{aligned} \tag{2.4}$$

The quantum $\boldsymbol{p}_{\mathrm{K,qu}}$ is a real vector; but in classically forbidden regions $E < U(\boldsymbol{r})$ the classical magnitude $p_{\mathrm{K,cl}}$ is imaginary, i.e. ${p_{\mathrm{K,cl}}}^2$ is negative.

The first equation in (2.3) expresses continuity of the probability density R^2, flowing with the quantum kinetic momentum $\boldsymbol{p}_{\mathrm{K,cl}}$. The second equation—the main interest here—shows that the quantum potential vanishes where the magnitude of the quantum kinetic momentum equals its classical counterpart:

$$Q(\mathbf{r}) = 0 \Rightarrow \left|\mathbf{p}_{\mathrm{K,qu}}(\mathbf{r})\right| = p_{\mathrm{K,cl}}(\mathbf{r})\,. \tag{2.5}$$

Obviously, this can only be satisfied in classically allowed regions, where $p_{\mathrm{K,cl}}(\boldsymbol{r})$ is real. For general potentials, ψ is not band-limited, so consideration of superoscillations is strictly premature. Nevertheless (2.5) and (2.4) have a similar interpretation: in classically allowed regions, $Q(\boldsymbol{r})$ can be positive, so according to (2.3) quantum waves vary more slowly than their semiclassical (WKB) approximation; or $Q(\boldsymbol{r})$ can be negative, so quantum waves vary faster than semiclassical. (In classically forbidden regions, $Q(\boldsymbol{r})$ is always negative; an instructive example for students is to calculate Q for the wave $\psi(x,y)=\exp\left(\mathrm{i}qx-y\sqrt{1+q^2}\right)$, which satisfies $\nabla^2\psi-\psi=0$, corresponding to negative energy and no forces).

The superoscillation phenomenon enters for the case of a uniform medium, where propagating waves satisfy the Helmholtz equation with constant wavenumber k_0:

$$\nabla^2\psi(\mathbf{r})+k_0^2\psi(\mathbf{r})=0. \tag{2.6}$$

Solutions that are superpositions of propagating (i.e nonevanescent) plane waves are band-limited, in the full $\boldsymbol{r}$ space or on any plane surface or straight line. This is because the wavevectors of all the plane waves have the same length k_0, and differ only in direction. The quantum kinetic momentum becomes the local wavevector:

$$\mathbf{k}(\mathbf{r})\equiv\nabla\arg\psi(\mathbf{r})=\mathrm{Im}\,\nabla\log\psi(\mathbf{r})=\mathrm{Im}\,\frac{\nabla\psi(\mathbf{r})}{\psi(\mathbf{r})}, \tag{2.7}$$

with at least five interpretations [7].

Superoscillations correspond to regions where the length of the local wavevector exceeds the wavenumber k_0 of all plane waves comprising the wave. And the vanishing of the quantum potential for the wave corresponds to the boundaries of such regions, given by a special case of (2.5):

$$|\mathbf{k}(\mathbf{r})|=k_0. \tag{2.8}$$

This establishes the claimed connection between quantum potential zeros and superoscillation boundaries.

3. Superoscillatory superpositions of plane waves

To create a solution of (2.6) in the plane $\boldsymbol{r}=(x,y)$, we start with a superoscillatory function on the x axis, and choose $k_0=1$, corresponding to wavelength $\lambda=2\pi$ (or, equivalently, measuring distances in units of $\lambda/2\pi$). For the function, we choose what has become the canonical and well-understood $2N\pi$-periodic superoscillation [8, 9]:

$$\begin{aligned}\psi(x,0)&=\left(\cos\left(\frac{x}{2N}\right)+\mathrm{i}a\ \sin\left(\frac{x}{2N}\right)\right)^{2N}=\sum_{n=-N}^{N}c_n\ \exp\left(\mathrm{i}\frac{nx}{N}\right)\\ c_n&=\frac{(2N!)\,(-1)^{N+n}\left(a^2-1\right)^N}{4^N\,(N+n)!\,(N-n)!}\left(\frac{a+1}{a-1}\right)^n\cdot\quad(a>1,\ N\ \text{integer})\end{aligned} \tag{3.1}$$

The parameter a represents the degree of superoscillation: for $x(\mathrm{Mod}(2\pi N))$ small, $\psi(x,0)\approx\exp(\mathrm{i}ax)$, so the local oscillations are faster by a than the oscillation $\exp(\pm\mathrm{i}x)$ corresponding to the Fourier extremes of the spectrum in (3.1). The integer N parameterises the number of superoscillations $\left(O\left(\sqrt{N}\right)\right)$ near $x=0$. Figure 1 illustrates the function, using the familiar [8] device of plotting the logarithm of the modulus of the real part to show the oscillations and

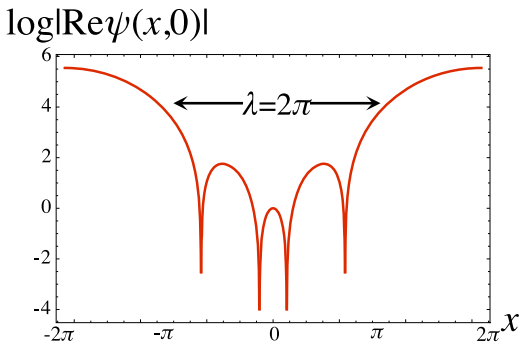

Figure 1. The superoscillatory function (3.1) for $a = 4$, $N = 2$. The horizontal bar indicates the period to be anticipated from the extreme wavenumbers ± 1 in the spectrum. The negative spikes represent zeros of Re ψ; in one wavelength there are four, instead of the two expected for cos x.

accommodate the large variation between the superoscillatory and non-oscillatory regions; the imaginary part looks similar. The reason for choosing the modest value $N = 2$ will be explained later.

To create the wave $\psi(x, y)$ in the plane, we extend each Fourier component away from the x axis, to form a band-limited superposition of nonevanescent plane waves:

$$\psi(x,y) = \sum_{n=-N}^{N} c_n \ \exp\left(\mathrm{i}\left(x\frac{n}{N} + y(-1)^n\sqrt{1-\left(\frac{n}{N}\right)^2}\right)\right). \tag{3.2}$$

The factor $(-1)^n$ is chosen to include plane waves travelling in both the $+y$ and $-y$ directions.

Figure 2 illustrates several different aspects of the geometry of this wave on different scales, for $a = 4$ and $N = 2$. In each picture, the thick red curves, satisfying (2.8) with $k_0 = 1$, are the zeros of the quantum potential, bounding the superoscillatory regions, shaded grey. The black dots in these regions indicate the singularities of the wave: nodal points, where the wavefronts (full black lines at phase intervals $\pi/4$) cross, and around which the phase gradient streamlines (curves with arrows) circulate. The occurrence of phase singularites, each representing an extreme of superoscillation, and their interpretation as wave vortices, are well understood [10, 11]; and for random superpositons of plane waves the fraction of the plane within the superoscillatory regions has been calculated [12, 13].

Figure 2(a) shows a square whose side length is one x period (the wave (3.2) is periodic in x but not y). There are 10 phase singularities. Two of them lie close together in the superoscillatory region of the x axis and are hard to resolve. The magnification in figure 2(b) shows the fine detail in this region. As in all cases, ψ is relatively very small where it superoscillates; for the wave (3.2), $|\psi| \sim 1$ in the superoscillatory region, rising to $|\psi| \sim a^{2N}$ elsewhere. Even for the modest value $N = 2$, $a^{2N} = 256$; as N increases, the disparity rises exponentially, and resolving the detail gets more difficult. Figure 2(c) shows the neighbourhood of one of the typical phase singularities away from the superoscillatory region.

The form of the zero-potential curves is similar near all the singularities. This is a consequence of the anisotropy of the pattern of wavefronts that meet at the singularity, or alternatively the anisotropy of the contours of $|\psi|$ surrounding the nodal point. The simplest model

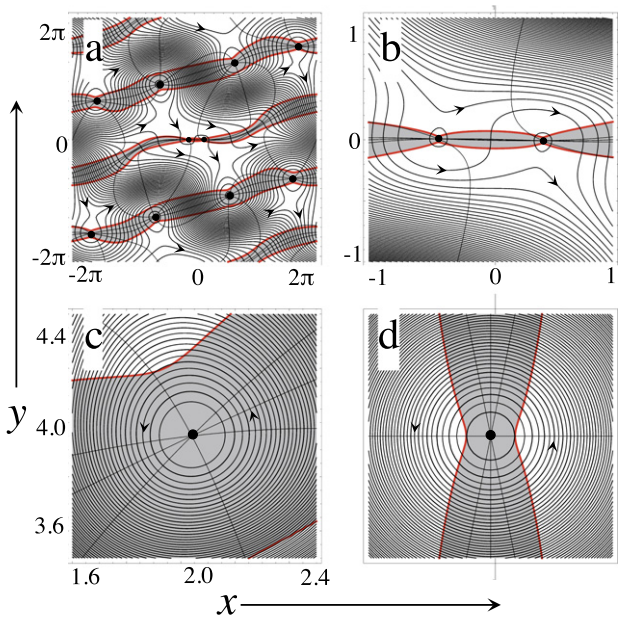

Figure 2. Geometry of the wave (3.2) (a–c), and the model (3.3) (d). Thick red curves: zero quantum potential contours; black dots: phase singularities; black curves: phase contours at $\pi/4$ intervals; curves with arrows: streamlines, i.e. integral curves of the local momentum field $\boldsymbol{k}(\boldsymbol{r})$; the superoscillatory regions are shaded grey.

displaying this behaviour, illustrated in figure 2(d), is

$$\psi(\mathbf{r}) = x + \mathrm{i}\varepsilon y, \quad \text{i.e. } |\psi(\mathbf{r})| = \sqrt{x^2 + \varepsilon^2 y^2}. \tag{3.3}$$

From (2.6), the local wavevector and its length are

$$\mathbf{k}(\mathbf{r}) = \frac{\varepsilon}{x^2 + \varepsilon^2 y^2}\left(-y\mathbf{e}_x + x\mathbf{e}_y\right), \quad |\mathbf{k}(\mathbf{r})| == \frac{\varepsilon\sqrt{x^2 + y^2}}{x^2 + \varepsilon^2 y^2}. \tag{3.4}$$

Therefore the streamlines are circles [14], and the distance of the zero-potential contour from the singularity is ε in the x direction and $1/\varepsilon$ in the y direction. In polar coordinates, the zero potential contour is

$$r(\theta) = \frac{\varepsilon}{\cos^2\theta + \varepsilon^2 \sin^2\theta}. \tag{3.5}$$

Figure 2(d), drawn for $\varepsilon = 0.2$, shows only part of this contour, which closes far away, in regions where the local approximation (3.3) fails.

4. AB waves

In the AB effect [15–17], quantum charged particles are influenced by a magnetic field concentrated into a single line of flux Φ. In the Schrödinger equation (2.1), there is no scalar potential, and Φ is represented by a vector potential. In the convenient circular gauge, and polar coordinates in the plane, and again scaling energy by measuring distances in units of $\lambda/2\pi$, (2.1) can

be written in terms of the dimensionless flux α:

$$\left(\nabla - \frac{\mathrm{i}\alpha}{r}\mathbf{e}_\theta\right)^2 \psi_0(\mathbf{r}) + \psi_0(\mathbf{r}) = 0, \quad \mathbf{r} = \{r\cos\theta, r\sin\theta\}, \quad \alpha = \frac{q\Phi}{\hbar}. \tag{4.1}$$

Singlevalued elementary solutions are

$$\psi_m(\mathbf{r}) = J_{|m-\alpha|}(r)\exp(\mathrm{i}m\theta), \tag{4.2}$$

and the celebrated AB wave [15], representing a plane wave incident from $x = -\infty$ and scattered by the flux line, is the superposition

$$\psi_{\mathrm{AB}}(\boldsymbol{r}) = \sum_{m=-\infty}^{\infty} (-\mathrm{i})^{|m-\alpha|}(-1)^m \psi_m(\boldsymbol{r}). \tag{4.3}$$

We are interested in the quantum potential zeros of these waves, which are curves determined by (2.5). To interpret these as the superoscillation boundary requires that ψ_m and ψ_{AB} are bandlimited. Strictly they are not. This is a subtle matter, involving technicalities discussed in the appendix. But since the wave outside the flux line moves in a plane free of electric and magnetic fields it is a reasonable extension of terminology describe the fast variations of these waves as superoscillations.

We write the kinetic momentum in (4.4) in terms of the 'kinetic wave vector'

$$\mathbf{k}_{\mathrm{K}}(\mathbf{r}) \equiv \frac{\mathbf{p}_{\mathrm{K,qu}}(\mathbf{r})}{\hbar}. \tag{4.4}$$

The streamlines defined by the direction of this vector for the AB wave (4.3) display fine detail very close to the flux line, as discussed recently [18] (and earlier [16]). The condition (2.5) for the quantum potential zeros, namely

$$|\mathbf{k}_{\mathrm{K}}(\mathbf{r})| = 1, \tag{4.5}$$

involves not the direction but the length of the vector, which was not studied before.

An alternative explanation of (4.5) deserves a brief description. The vector potential in (4.1) can be gauged away [16] by the substitution

$$\psi(\mathbf{r}) \Rightarrow \exp(-\mathrm{i}\alpha\theta)\,\psi(\mathbf{r}). \tag{4.6}$$

This new ψ satisfies the free-space Helmholtz equation (2.6) (with $k_0 = 1$). AB physics is incorporated by ψ being non-singlevalued if the quantum flux is non-integer: under continuation around a circuit of the flux line, ψ acquires a phase shift $-2\pi\alpha$. In this representation, $\boldsymbol{k}_{\mathrm{K}}(\boldsymbol{r})$ is simply the phase gradient as in (2.7). Gauge invariance implies [19] that AB observables in quantum physics must be periodic in the flux α. This is true of the wave (4.6) but is not true for the AB wave (4.3); although (4.3) is singlevalued under continuation around the flux line, the phase of this wave shifts by $2\pi\alpha$ as α increases by unity. However, the kinetic momentum $\boldsymbol{k}_{\mathrm{K}}(\boldsymbol{r})$ is periodic in α, and so it is in principle observable; it is a gauge-invariant vector, which was the reason for studying its streamlines [16, 18]. However, the wave equation (4.1) also describes the classical physics of waves in a vortex flow, with α representing the strength of the vortex, in a medium flowing much more slowly than the wave [20]. For such cases, the phase, although not periodic in α, is directly observable, and it was observed for water waves encountering a bathtub vortex [20] (for an extension of this idea to fast flows, see [21]).

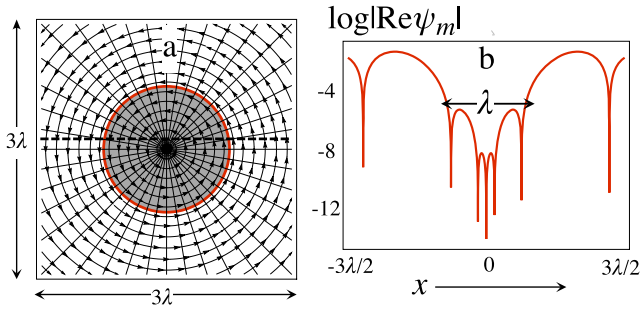

Figure 3. The elementary AB wave ψ_m (4.2) for $m = 5$, $\alpha = 1/4$. (a) Phase contours of ψ_m (thin black lines), streamlines circulating around the flux (curves with arrows), quantum potential zero (red curve), enclosing the superoscillatory region (grey). (b) Re ψ_m along the flyby of the flux line corresponding to the dashed black line in (a).

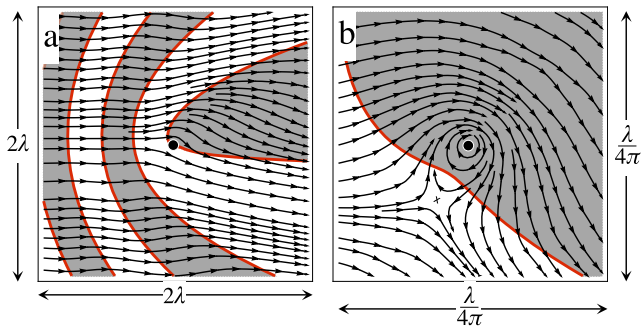

Figure 4. The AB wave for scattering from a flux line (black dots) with strength $\alpha = 1/4$, showing the quantum potential zeros (red curves), bounding the superoscillatory regions (grey), and the gauge-invariant streamlines (arrowed; these are the integral curves of the vector field $\boldsymbol{k}_{\mathrm{K}}$ in (4.7)); (a) large-scale view, showing the streamlines arriving from the left and being deviated by the flux line; (b) magnification showing the vortex (black dot)-saddle (x) structure [18] very close to the flux.

Now we return to the singlevalued solutions of (4.1), i.e. (4.2) and (4.3). In polar coordinates, for any solution ψ of (4.1)

$$\mathbf{k}_{\mathrm{K}}(\mathbf{r}) = \{k_{\mathrm{K}r}(\mathbf{r}), k_{\mathrm{K}\theta}(\mathbf{r})\} = \left\{\mathrm{Im}\ \frac{\partial_r\psi(\mathbf{r})}{\psi(\mathbf{r})}, \frac{1}{r}\left(\mathrm{Im}\ \frac{\partial_\theta\psi(\mathbf{r})}{\psi(\mathbf{r})} - \alpha\right)\right\}. \tag{4.7}$$

Consider first the elementary waves ψ_m. From (4.2),

$$k_{\mathrm{K}r} = 0, \quad k_{\mathrm{K}\theta} = \frac{m-\alpha}{r}. \tag{4.8}$$

Therefore the wavevector streamlines are circles, and the zero of the quantum potential is the circle $r = |m-\alpha|$. Figure 3(a) illustrates this geometry for $m = 5$, $\alpha = 1/4$. Figure 3(b) illustrates the wave (4.2) along the 'flyby' of the flux line corresponding to the dashed line in figure 3(a), showing the superoscillations near the phase singularity at the flux line.

For the AB superposition (4.3), the same quantities are easy to compute, and figure 4 illustrates the analogous behaviour. The red curves are the quantum potential zeros, bounding the

grey regions where the wave is superoscillatory, and the streamlines arrive from the left and are deviated when they encounter the flux line. Figure 4(a) is the large scale view. Before the encounter, the superoscillatory regions form bands, approximately $\lambda/4$ wide far from the flux line; within these bands, $|\boldsymbol{k}_{\mathrm{K}}|$ exceeds 1 only slightly, and between them it is only slightly less. In this view, the detail near the flux line is not resolved. The $8\pi \sim 25$ linear magnification in figure 4(b) shows the previously studied vortex/saddle geometry of the streamlines [16, 18], as well as the quantum potential zero curves bounding the superoscillatory region. The curves do not have the canonical form illustrated in figure 2(d), because although ψ_{AB} has a phase singularity at the flux line (whose strength is the nearest integer to α [20]), this wave is not smooth there, so the model (3.3) does not apply.

5. Concluding remarks

The connection reported here, between zeros of the quantum potential and the boundaries of superoscillatory regions, can be seen in a wider context that would be useful in graduate-level physics teaching: the intertwining of historical threads linking old ideas with current research. As I have explained elsewhere [22, 23], there is a sense in which the germ of the Madelung–Bohm representation of waves, incorporating the quantum potential, can be traced back to Isaac Newton's speculations about edge diffraction at the beginning of the 18th century.

Superoscillations are especially strong near phase singularities, which were first discovered by William Whewell in the early 19th century in the patterns of tides in the world's oceans [22, 24, 25], and are currently being extensively explored and applied, especially in optics [26, 27]. The modern exploration of superoscillations was triggered by Yakir Aharonov's 'weak measurements' in quantum physics [9, 28], although there were anticipations in radar theory in world war II [29, 30].

And of course Aharonov co-discovered the eponymous AB effect with David Bohm, in which, as argued here, there exists, close to the flux line, fine detail that can be regarded as superoscillation. Consideration of the AB effect, especially its singlevalued and multivalued representations, and the central role of the kinetic momentum, provides an entry into quantum gauge physics [19].

These historical connections provide an abundant illustration of the quotation by F C Frank at the bottom of the first page of this paper.

Acknowledgments

I thank Professor Gilberto Silva-Ortigoza for sending me a preprint of his paper with colleagues [3], which stimulated the research reported here, and for a helpful correspondence. My research is supported by an Emeritus Fellowship from the Leverhulme Trust.

Appendix. Bandlimitedness and AB waves

The best hope for bandlimitedness is the representation (4.6), in which AB waves, although not singlevalued, satisfy the free-space Helmholtz equation (2.6). It suffices to discuss the elementary waves (4.2); in the Helmholtz representation, these are

$$\psi(\mathbf{r}) = J_{|\nu|}(\mathbf{r}) \exp(\mathrm{i}\nu\theta), \quad (\nu = m - \alpha). \tag{A.1}$$

Like all solutions of Helmholtz, this can be represented as a superposition of plane waves travelling in different directions, all of whose wavevectors $\boldsymbol{q}$ have the length 1; from the Sommerfeld

integral representation of $J_{|\nu|}$ (e.g. 8.412.6 in [31]), followed by a shift of contour,

$$J_{|\nu|}(r)\exp(\mathrm{i}\nu\theta)=\frac{(-\mathrm{i})^{\nu}}{2\pi}\int_{C}\mathrm{d}\phi\ \exp(\mathrm{i}\phi\nu)\exp(\mathrm{i}\mathbf{q}(\phi)\cdot\mathbf{r}),\quad\{-\pi\leqslant\theta\leqslant\pi\},$$
$$\mathbf{q}(\phi)=\{\cos\phi,\sin\phi\},\quad\mathbf{r}=r\{\cos\theta,\sin\theta\},\quad C=\{\mathrm{i}\infty,0,2\pi,2\pi+\mathrm{i}\infty\}. \tag{A.2}$$

In the two complex legs of C, the plane waves have complex directions ϕ, so they are evanescent, rather than propagating, waves. For integer ν, the contributions of these legs cancel, and the superposition involves only propagating waves, so it is band-limited. But for noninteger ν, corresponding to nontrivial AB flux, there is no cancellation, so it seems these AB waves are not bandlimited.

However, we note the curious fact [32] that any evanescent wave can be expressed as the limit of a bandlimited function. One such representation is

$$\begin{aligned}\exp(\mathrm{i}ux)\exp\left(-y\sqrt{u^2-1}\right)&=\lim_{\Delta\to0}\frac{\sqrt{2\pi}}{\Delta}\ \exp\left(-\frac{1}{\Delta^2}\right)\\&\quad\times J_0\left(\left(x-\mathrm{i}\frac{u}{\Delta^2}\right)^2+\left(y+\frac{\sqrt{u^2-1}}{\Delta^2}\right)^2\right)\\&=\lim_{\Delta\to0}\frac{1}{\Delta\sqrt{2\pi}}\int_{-\pi}^{\pi}\mathrm{d}\phi\ \exp(\mathrm{i}(x\ \cos\phi+y\ \sin\phi))\\&\quad\times\exp\left(-\frac{2}{\Delta^2}\ \sin^2\left(\frac{1}{2}\left(\phi-\mathrm{i}\ \cosh^{-1}u\right)\right)\right)\end{aligned} \tag{A.3}$$

with $u>1$. The limit is very singular, in the sense that in order to well approximate the evanescent wave the value of Δ must get rapidly smaller as x or y increase. I do not know whether there is a rigorous mathematical sense in which the limit can be invoked to claim that the AB wave is bandlimited.

Finally, another curiosity appears if one notes that the multivalued function (A.1) is singlevalued on the covering space $-\infty<\theta<\infty$, and then interprets the Fourier transform as an integral over all windings:

$$\bar{\psi}(q,\phi)=\int_0^{\infty}\mathrm{d}r\ rJ_{|\nu|}(r)\,\frac{1}{2\pi}\int_{-\infty}^{\infty}\mathrm{d}\theta\ \exp(\mathrm{i}\nu\theta)\exp(\mathrm{i}qr\ \cos(\theta-\phi)). \tag{A.4}$$

Splitting the angular integration into separate windings (intervals of length 2π) gives

$$\begin{aligned}\frac{1}{2\pi}\int_{-\infty}^{\infty}\mathrm{d}\theta\exp(\mathrm{i}\nu\theta)\exp(\mathrm{i}qr\cos(\theta-\phi))&=\frac{\exp(\mathrm{i}\nu\phi)}{2\pi}\int_{-\infty}^{\infty}\mathrm{d}u\exp(\mathrm{i}\nu u)\exp(\mathrm{i}qr\cos u)\\&=\frac{\exp(\mathrm{i}\nu\phi)}{2\pi}\sum_{m=-\infty}^{\infty}\int_{2m\pi}^{2(m+1)\pi}\mathrm{d}u\exp(\mathrm{i}\nu u)\exp(\mathrm{i}qr\cos u)\\&=\frac{\exp(\mathrm{i}\nu\phi)}{2\pi}\sum_{m=-\infty}^{\infty}\exp(2\pi\mathrm{i}m\nu)\int_0^{2\pi}\mathrm{d}u\exp(\mathrm{i}\nu u)\exp(\mathrm{i}qr\cos u)\\&=\exp(\mathrm{i}\nu\phi)\sum_{n=-\infty}^{\infty}\delta(\nu-n)J_n(qr).\end{aligned} \tag{A.5}$$

Thus the Fourier transform (A.4) becomes

$$\begin{aligned}\bar{\psi}(q,\phi) &= \exp(\mathrm{i}\nu\phi)\sum_{n=-\infty}^{\infty}\delta(\nu-n)\int_0^\infty \mathrm{d}r\; rJ_n(r)J_n(qr)\\ &= \exp(\mathrm{i}\nu\phi)\sum_{n=-\infty}^{\infty}\delta(\nu-n)\lim_{R\to\infty}\frac{R\left(J_{n+1}(R)J_n(qR)-qJ_n(R)J_{n+1}(qR)\right)}{1-q^2}\\ &= \exp(\mathrm{i}\nu\phi)\sum_{n=-\infty}^{\infty}\delta(\nu-n)\,\delta(q-1)\,,\end{aligned} \tag{A.6}$$

where the final equality follows from the asymptotic expansion of the Bessel functions for R large and q near 1. This is certainly band-limited: the Fourier transform contains only real plane waves with the free space wavenumber 1. But the sum over windings has eliminated all the fractional fluxes that are the essence of the AB effect.

ORCID iDs

M V Berry https://orcid.org/0000-0001-7921-2468

References

[1] Madelun E 1927 Quantentheorie in hydrodynamische form *Z. Phys.* **40** 322–6
[2] Holland P 1993 *The quantum theory of motion: An account of the de Broglie Bohm causal interpretation of quantum mechancis* (Cambridge: Cambridge University Press)
[3] Espíndola-Ramos E, Silva-Ortigoza G, Sosa-Sánchez C T, Julián-Mácias I, Gonzalez-Juárez A, Cabrera-Rosas O d J, Ortega-Vidals P, Rickenstorff-Parrao C and Silva-Ortigoza R 2020 Characterization of quantum waves: comparison between the caustic and the zeros of the Madelung–Bohm potential *J. Opt. Soc. Am.* (submitted)
[4] Berry M V 1994 Faster than Fourier *Quantum Coherence and Reality celebration of the 60th Birthday of Yakir Aharonov* ed J S Anandan and J L Safko (Singapore: World Scientific) pp 55–65
[5] Aharonov Y, Colombo F, Sabadini I, Struppa D and Tollaksen J 2017 The mathematics of superoscillations *Mem. Am Math. Soc.* **247** 1174
[6] Berry M *et al* 2019 Roadmap on superoscillations *J. Opt.* **21** 053002
[7] Berry M V 2013 Five momenta *Eur. J. Phys.* **34** 1337–48
[8] Berry M V and Popescu S 2006 Evolution of quantum superoscillations and optical superresolution without evanescent waves *J. Phys. A: Math. Gen.* **39** 6965–77
[9] Aharonov Y, Popescu S and Tollaksen J 2010 A time-symmetric formulation of quantum mechanics *Phys. Today* **63** 27–32
[10] Berry M V 2008 Waves near zeros *Coherence and Quantum Optics* ed N P Bigelow, J H Eberly and C R J Stroud (Washington DC: Optical Society of America) pp 37–41
[11] Berry M V 2013 A note on superoscillations associated with Bessel beams *J. Opt.* **15** 044006
[12] Dennis M R, Hamilton A C and Courtial J 2008 Superoscillation in speckle patterns *Opt. Lett.* **33** 2976–8
[13] Berry M V and Dennis M R 2009 Natural superoscillations in monochromatic waves in D dimensions *J. Phys. A: Math. Theor.* **42** 022003
[14] Berry M V and Dennis M R 2000 Phase singularities in isotropic random waves *Proc. R. Soc.* A **456** 2059–79
Berry M V and Dennis M R 2000 Phase singularities in isotropic random waves *Proc. R. Soc.* A **456** 3048 (corrigenda)
[15] Aharonov Y and Bohm D 1959 Significance of electromagnetic potentials in the quantum theory *Phys. Rev.* **115** 485–91

[16] Olari S and Popescu I I 1985 The quantum effects of electromagnetic fluxes *Revs. Mod. Phys.* **57** 339–436
[17] Peshkin M and Tonomura A 1989 *The Aharonov–Bohm Effect* (*Springer Lecture Notes in Physics* vol 430) (Berlin: Springer)
[18] Berry M V 2017 Gauge-invariant Aharonov–Bohm streamlines *J. Phys. A: Math. Theor.* **50** 43LT01
[19] Wu T T and Yang C N 1975 Concept of nonintegrable phase factors and global formulation of gauge fields *Phys. Rev.* D **12** 3845–57
[20] Berr M V, Chambers R G, Large M D, Upstill C and Walmsley J C 1980 Wavefront dislocations in the Aharonov–Bohm effect and its water-wave analogue *Eur. J. Phys.* **1** 154–62
[21] Torrres T, Patrick S, Coutant A, Richartz M, Tedford E W and Weinfurtner S 2017 Observation of superradiance in a vortex flow *Nat. Phys.* **13** 833–6
[22] Berry M V 2002 Exuberant interference: rainbows, tides, edges, (de)coherence *Phil. Trans. R. Soc.* A **360** 1023–37
[23] Berry M 2017 Approaches to studying our history *Phys. Today* **70** 11–2
[24] Whewell W 1833 Essay towards a first approximation to a map of cotidal lines *Phil. Trans. Roy. Soc.* **123** 147–236
[25] Whewell W 1836 On the results of an extensive series of tide observations made on the coasts of Europe and America in June 1835 *Phil. Trans. Roy. Soc.* **126** 289–341
[26] Ny J F 1999 *Natural Focusing and Fine Structure of Light: Caustics and Wave Dislocations* (Bristol: Institute of Physics Publishing)
[27] Rubinsztein-Dunlop H *et al* 2017 Roadmap on structured light *J. Opt.* **19** 013001
[28] Aharonov Y, Albert D Z and Vaidman L 1988 How the result of a measurement of a component of the spin of a spin-1/2 particle can turn out to be 100 *Phys. Rev. Lett.* **60** 1351–4
[29] Schelkunoff S A 1943 A mathematical theory of linear arrays *Bell Syst. Tech. J.* **22** 80–107
[30] Berry M V 2013 Superoscillations, endfire and supergain *Quantum Theiory: A Two-Time Success Story: Yakir Aharonov Festschrift* ed D Struppa and J Tollaksen (New York: Springer) pp 327–36
[31] Gradshteyn I S and Ryzhik I M 1980 *Table of Integrals, Series and Products* (New York: Academic)
[32] Berry M V 1994 Evanescent and real waves in quantum billiards and Gaussian beams *J. Phys. A: Math. Gen.* **27** L391–8